Optimal control of two-commercial aircraft dynamic system during approach

Fulgence Nahayo, Salah Khardi, Mounir Haddou

Optimal control of two-commercial aircraft dynamic system during approach. The noise levels minimization

F. Nahayo[1,2], S. Khardi[2] and M. Haddou[3]

[1] University Claude Bernard of Lyon 1 (France) and University
of Burundi (Burundi), E-Mail: fulgence.nahayo@ifsttar.fr
[2] The French Institute of Science and Technology for Transport,
Development and Networks - Transport and Environment
Laboratory, Lyon - France, E-Mail: salah.khardi@ifsttar.fr
[3] University of Orléans. CNRS-MAPMO, France,
E-Mail: mounir.haddou@univ-orleans.fr

Abstract

This paper aims to reduce noise levels of two-aircraft landing simultaneously on approach. Constraints related to stability, performance and flight safety are taken into account. The problem of optimal control is described and solved by a Sequential Quadratic Programming numerical method 'SQP' when globalized by the trust region method. By using a merit function, a sequential quadratic programming method associated with global trust regions bypasses the non-convex problem. This method used a nonlinear interior point trust region optimization solver under AMPL. Among several possible solutions, it is shown that there is an optimal trajectory leading to a reduction of noise levels on approach.

1   Introduction

The aim of this work is the development of a theoretical model of noise optimization while maintaining a reliable evolution of the flight procedures of two commercial aircraft on approach. These aircraft are supposed to land successively on one runway without conflict [37]. It is all about the evolution of flight dynamics and minimization of noise for two similar commercial aircraft landing taking into account the energy constraint. This model is a non-linear and non-convex optimal control. It is governed by a system of ordinary non-linear differential equations [12]. The 3-D movement of the two planes is described by a system depending on ordinary non-linear differential equations with mixed constraints. The function to be minimized is the integral describing the overall level of noise emitted by the two aircraft on approach and collected on the ground. We take into account constraints related to joint stability, performance and flight safety.

The problem of optimal control is described and solved by a Trust Region Sequential Quadratic Programming method 'TRSQP'[3, 5, 10, 11, 30]. By using a merit function, a sequential quadratic programming method associated with global trust regions bypasses the non-convex problem. This method is established by following a tangent quadratic problem obtained from the optimality conditions of Karush-Khun-Tucker applied to the problem considering the objective function as the merit function.

The TRSQP methods are suggested as an option by a Nonlinear Interior point Trust Region Optimization solver 'KNITRO' [33] under A Mathematical Programming Modeling Language 'AMPL'[17, 27]. The global convergence properties are analyzed under different assumptions on the approximate Hessian. Additional assumptions on the feasibility perturbation technique are used to prove quadratic convergence to points satisfying second-order sufficient conditions.

Details of the two-aircraft flight dynamic, the noise levels, the constraints, the mathematical model of the two-aircraft acoustic optimal control problem and the trust region sequential quadratic programming method processing are presented in section 2, 3 and 4 while the numerical experiments are presented in the last section.

2   Mathematical Modelization

The motion of each aircraft $A_i, i := 1, 2$ is three dimensional analyzed with 3 frames: the landmark $(O, \overrightarrow{X}_1, \overrightarrow{Y}_1, \overrightarrow{Z}_1)$, the aircraft frame $(G_i, \overrightarrow{X}_{Gi}, \overrightarrow{Y}_{Gi}, \overrightarrow{Z}_{Gi})$ and the aerodynamic one $(G_i, \overrightarrow{X}_{ai}, \overrightarrow{Y}_{ai}, \overrightarrow{Z}_{ai})$ where $i := 1, 2$ [6]. The transition between these three frames is shown easily [7]. In general, the equations of

motion of each aircraft are summarized as:

$$\begin{aligned}
\sum \overrightarrow{F}_{ext_i} - \frac{dm_i}{dt}\overrightarrow{V}_{a_i} &= \frac{m_i d\overrightarrow{V}_{a_i}}{dt} \\
\sum \overrightarrow{M}_{ext_{G_i}} &= \frac{d}{dt}[I_{G_i}\overrightarrow{\Omega}_i] \\
\frac{d\overrightarrow{X}^o}{dt} &= \frac{d\overrightarrow{X}^1}{dt} + \overrightarrow{\Omega}_{10} \times \overrightarrow{X}
\end{aligned} \tag{1}$$

The index i = 1, 2 reflects the aircraft. In the system above, $\overrightarrow{F}_{ext_i}$ represents the external forces acting on the aircraft, $m_i(t)$ the mass of the aircraft, v_i the airspeed of aircraft, $\overrightarrow{M}_{ext_{G_i}}$ the moments of each aircraft, $J(G_i, A_i)$ the inertia matrix, $\frac{d\overrightarrow{X}^o}{dt}$ is the derivative with respect to time of the vector X in vehicle-carried normal Earth frame R_O, $\frac{d\overrightarrow{X}^1}{dt}$ is the derivative with respect to time of the vector X in frame R_1, Ω_i the angular rotation of the aircraft and Ω_{10} is the angular velocity of the frame R_1 relative to the frame R_O. After transformations and simplifications, the system (1) becomes:

$$\begin{cases}
\dot{V}_{a_i} &= \frac{1}{m_i}[-m_i g sin\gamma_{a_i} - \frac{1}{2}\rho S V_{a_i}^2 C_D \\
&\quad + (cos\alpha_{a_i}cos\beta_{a_i} + sin\beta_{a_i} + sin\alpha_{a_i}cos\beta_{a_i})F_{x_i} - \frac{dm_i}{dt}u_i - m_i\Delta A_u^i] \\
\dot{\beta}_{a_i} &= \frac{1}{m_i V_{a_i}}[m_i g cos\gamma_{a_i}sin\mu_{a_i} + \frac{1}{2}\rho S V_{a_i}^2 C_{y_i} \\
&\quad + [-cos\alpha_{a_i}sin\beta_{a_i} + cos\beta_{a_i} - sin\alpha_{a_i}sin\beta_{a_i}]F_{y_i} - \frac{dm_i}{dt}v_i - m_i\Delta A_v^i] \\
\dot{\alpha}_{a_i} &= \frac{1}{m_i V_{a_i}cos\beta_{a_i}}[m_i g cos\gamma_{a_i}cos\mu_{a_i} - \frac{1}{2}\rho S V_{a_i}^2 C_{L_i} + [-sin\alpha_{a_i} + cos\alpha_{a_i}]F_{z_i} \\
&\quad - \frac{dm_i}{dt}w_i - m_i\Delta A_w^i] \\
\dot{p}_i &= \frac{C}{AC-E^2}\{r_i q_i(B-C) - Ep_i q_i + \frac{1}{2}\rho S l V_{a_i}^2 C_{l_i} \\
&\quad + \sum_{j=1}^2 F_j[y_{M_{ij}}^b cos\beta_{m_{ij}}sin\alpha_{m_{ij}} - z_{M_{ij}}^b sin\beta_{m_{ij}}]\} \\
&\quad + \frac{E}{AC-E^2}\{p_i q_i(A-B) - Er_i q_i + \frac{1}{2}\rho S l V_{a_i}^2 C_{ni} \\
&\quad + \sum_{j=1}^2 F_j[x_{M_{ij}}^b sin\beta_{m_{ij}} - y_{M_{ij}}^b cos\beta_{m_{ij}}cos\alpha_{m_{ij}}]\} \\
\dot{q}_i &= \frac{1}{B}\{-r_i p_i(A-C) - E(p_i^2 - r_i^2) + \frac{1}{2}\rho S l V_{a_i}^2 C_{mi} \\
&\quad + \sum_{j=1}^2 F_j[z_{M_{ij}}^b cos\beta_{m_{ij}}cos\alpha_{m_{ij}} - x_{M_{ij}}^b cos\beta_{m_{ij}}sin\alpha_{m_{ij}}]\} \\
\dot{r}_i &= \frac{E}{AC-E^2}\{r_i q_i(B-C) + Ep_i q_i + \frac{1}{2}\rho S l V_{a_i}^2 C_{l_i} \\
&\quad + \sum_{j=1}^2 F_j[y_{M_{ij}}^b cos\beta_{m_{ij}}sin\alpha_{m_{ij}} - z_{M_{ij}}^b sin\beta_{m_{ij}}]\} \\
&\quad + \frac{A}{AC-E^2}\{p_i q_i(A-B) - Er_i q_i + \frac{1}{2}\rho S l V_{a_i}^2 C_{ni} \\
&\quad + \sum_{j=1}^2 F_j[x_{M_{ij}}^b sin\beta_{m_{ij}} - y_{M_{ij}}^b cos\beta_{m_{ij}}cos\alpha_{m_{ij}}]\} \\
\dot{X}_{G_i} &= V_{a_i}cos\gamma_{a_i}cos\chi_{a_i} + u_w \\
\dot{Y}_{G_i} &= V_{a_i}cos\gamma_{a_i}sin\chi_{a_i} + v_w \\
\dot{Z}_{G_i} &= -V_{a_i}sin\gamma_{a_i} + w_w \\
\dot{\phi}_i &= p_i + q_i sin\phi_i tan\theta_i + r_i cos\phi_i tan\theta_i \\
\dot{\theta}_i &= q_i cos\phi_i - r_i sin\phi_i \\
\dot{\psi}_i &= \frac{sin\phi_i}{cos\theta_i}q_i + \frac{cos\phi_i}{cos\theta_i}r_i \\
\dot{m}_i &= -2.01 \times 10^{-5}\frac{(\Phi-\mu-\frac{K}{\eta_c})\sqrt{\Theta}}{\sqrt{5\eta_n(1+\eta_{tf}\lambda)}\sqrt{G+0.2M^2\frac{\eta_d}{\eta_{tf}}\lambda-(1-\lambda)M}}\frac{1}{2}\rho S V_{ai}^2 C_D
\end{cases} \tag{2}$$

where j means the engine index, the expressions $A = I_{xx}, B = I_{yy}, C = I_{zz}, E = I_{xz}$ are the inertia moments of the aircraft, ρ is the air density, S is the aircraft reference area, l is the aircraft reference length, g is the acceleration due to gravity, $C_D = C_{D0} + kC_L^2$ is the drag coefficient, $C_{yi} = C_{y\beta}\beta + C_{yp}\frac{pl}{V} + C_{yr}\frac{rl}{V} + C_{Y\delta_l}\delta_l + C_{Y\delta_n}\delta_n$ is the lateral forces coefficient, $C_{Li} = C_{L\alpha}(\alpha_a - \alpha_{a0}) + C_{L\delta_m}\delta_m + C_{LM}M + C_{Lq}\frac{q_a^b l}{V}$ is the lift coefficient, $C_{li} = C_{l\beta}\beta + C_{lp}\frac{pl}{V} + C_{lr}\frac{rl}{V} + C_{l\delta_l}\delta_l + C_{l\delta_n}\delta_n$ is the rolling moment coefficient, $C_{mi} = C_{m0} + C_{m\alpha}(\alpha - \alpha_0) + C_{m\delta_m}\delta_m$ is the pitching moment coefficient, $C_{ni} = C_{n\beta}\beta + C_{np}\frac{pl}{V} + C_{nr}\frac{rl}{V} + C_{n\delta_l}\delta_l + C_{n\delta_n}\delta_n$ is the yawing moment coefficient, $(x_{Mij}^b, x_{Mij}^b, x_{Mij}^b)$ is the position of the engine in the body frame, $F = (F_{xi}, F_{yi}, F_{zi})$ is the propulsive force, $V_{ai} = (u_i, v_i, w_i)$ is the aerodynamic speed, $(\Delta A_u^i, \Delta A_v^i, \Delta A_w^i)$ is the complementary acceleration, (u_w, v_w, w_w) is the wind velocity, β_{mij} is the yaw setting of the engine and α_{mij} is the pitch setting of the engine. The mass change is reflected in the aircraft fuel consumption as described by E. Torenbeek [36] where the specific consumption is

$$C_{SR_i} = 2.01 \times 10^{-5} \frac{(\Phi - \mu - \frac{K_i}{\eta_c})\sqrt{\Theta}}{\sqrt{5\eta_n(1 + \eta_{tf_i}\lambda)}\sqrt{G_i + 0.2M_i^2\frac{\eta_{d_i}}{\eta_{tf_i}}\lambda - (1 - \lambda)M_i}}$$

with the generator function G:

$$\begin{aligned} G_i &= (\Phi - \frac{K_i}{\eta_c})(1 - \frac{1.01}{\eta_i^{\frac{\nu-1}{\nu}}(K_i + \mu_i)(1 - \frac{K_i}{\Phi\eta_c\eta_t})}) \\ K_i &= \mu_i(\epsilon_c^{\frac{\nu-1}{\nu}} - 1) \\ \mu_i &= 1 + \frac{\nu-1}{2}M_i^2 \end{aligned}$$

The Nomenclature of engine performance variables are given by G the gas generator power function, G0 the gas generator power function (static, sea level), K_i the temperature function of compression process, M_i the flight Mach number, T4 the turbine Entry total Temperature, T0 the ambient temperature at sea level, T the flight temperature, while the nomenclature of engines yields is $\eta_c = 0.85$ the isentropic compressor efficiency, $\eta_{d_i} = 1 - 1.3(\frac{0.05}{Re^{\frac{1}{5}}})^2(\frac{0.5}{M_i})^2\frac{L}{D}$, the isentropic fan intake duct efficiency, L the duct length, D the inlet diameter, Re the reynolds number at the entrance of the nozzle, $\eta_{f_i} = 0.86 - 3.13 \times 10^{-2}M_i$ the isentropic fan efficiency, $\eta_i = \frac{1 + \eta_{d_i}\frac{\gamma-1}{2}M_i^2}{1 + \frac{\gamma-1}{2}M_i^2}$ the gas Generator intake stagnation pressure ratio, $\eta_n = 0.97$ the isentropic efficiency of expansion process in nozzle, $\eta_t = 0.88$ the isentropic turbine efficiency $\eta_{tf_i} = \eta_t\eta_{f_i}$, ϵ_c the overall pressure ratio (compressor), ν the ratio of specific heats $\nu = 1.4$, λ the bypass ratio, μ_i the ratio of stagnation to static temperature of ambient air, Φ the nondimensional turbine entry temperature $\Phi = \frac{T_4}{T}$ and Θ the relative ambient temperature $\Theta = \frac{T}{T_0}$. The expressions $\alpha_{ai}(t), \beta_{ai}(t), \theta_i(t), \psi_i(t), \phi_i(t), V_{a_i}(t), X_{G_i}(t), Y_{G_i}(t), Z_{G_i}(t), p_i(t), q_i(t), r_i(t), m_i(t)$

are respectively the attack angle, the aerodynamic sideslip angle, the inclination angle, the cup, the roll angle, the airspeed, the position vectors, the roll velocity of the aircraft relative to the earth, the pitch velocity of the aircraft relative to the earth, the yaw velocity of the aircraft relative to the earth and the aircraft mass.

Transforming the system (2) in state function, one has:

$$\frac{dy_i(t)}{dt} = f_i(y_i(t), u_i(t)), i = 1, 2 \tag{3}$$

where the state vector is:

$$
\begin{aligned}
y_i(t) \quad &: [t_0, t_f] \longrightarrow \mathbf{R}^{13} \\
y_i(t) \quad &= (\alpha_{ai}(t), \beta_{ai}(t), \theta_{ai}(t), \psi_{ai}(t), \phi_i(t), V_{a_i}(t), X_{G_i}(t), Y_{G_i}(t), Z_{G_i}(t), p_i(t), \\
&\quad q_i(t), r_i(t), m_i(t))
\end{aligned}
\tag{4}
$$

The control vector is

$$
\begin{aligned}
u_i(t) &: [t_0, t_f] \longrightarrow \mathbf{R}^4 \\
t &\longrightarrow u_i(t) = (\delta_{l_i}(t), \delta_{m_i(t)}, \delta_{n_i}(t), \delta_{x_i}(t))
\end{aligned}
\tag{5}
$$

where the expressions $\delta_{l_i}(t), \delta_{m_i(t)}, \delta_{n_i}(t), \delta_{x_i}(t)$ are respectively the roll control, the pitch control, the yaw control and the thrust one. The dynamics relationship can be written as:

$$\dot{y}_i(t) = f_i(y_i(t), u_i(t), t), \forall t \in [0, T], y_i(0) = y_{i0} \tag{6}$$

The angles $\gamma_{a_i}(t), \chi_{a_i}(t), \mu_{a_i}(t)$ corresponding respectively to the aerodynamic climb angle (air-path inclination angle), the aerodynamic azimuth (air-path track angle) and the air-path bank angle (aerodynamic bank angle) are not taken as state in this model.

To simplify the model, the atmosphere standards conditions are considered. The engine angles, the complementary acceleration and the aerodynamic sideslip angle are negligible because the wind is constant and there is no engine failure. With some complex mathematical transformations, the dynamic

system (2) becomes:

$$
\begin{cases}
\dot{V}_{a_i} & = \frac{1}{m_i}[-m_i g sin\gamma_{a_i} - \frac{1}{2}\rho S V_{a_i}^2 C_D + (cos\alpha_{a_i} + sin\alpha_{a_i})F_{x_i} - \dot{m}_i u_i] \\
\dot{\alpha}_{a_i} & = \frac{1}{m_i V_{a_i} cos\beta_{a_i}}[m_i g cos\gamma_{a_i} cos\mu_{a_i} - \frac{1}{2}\rho S V_{a_i}^2 C_{L_i} \\
& \quad + [cos\alpha_{a_i} - sin\alpha_{a_i}]F_{z_i} - \dot{m}_i w_i] \\
\dot{p}_i & = \frac{C}{AC-E^2}\{r_i q_i(B-C) - Ep_i q_i + \frac{1}{2}\rho Sl V_{a_i}^2 C_{l_i}\} \\
& \quad + \frac{E}{AC-E^2}\{p_i q_i(A-B) - Er_i q_i + \frac{1}{2}\rho Sl V_{a_i}^2 C_{ni} \\
\dot{q}_i & = \frac{1}{B}\{-r_i p_i(A-C) - E(p_i^2 - r_i^2) + \frac{1}{2}\rho S_i l V_{a_i}^2 C_{mi}\}, \\
\dot{r}_i & = \frac{E}{AC-E^2}\{r_i q_i(B-C) + Ep_i q_i + \frac{1}{2}\rho Sl V_{a_i}^2 C_{l_i} \\
& \quad + \frac{A}{AC-E^2}\{p_i q_i(A-B) - Er_i q_i + \frac{1}{2}\rho Sl V_{a_i}^2 C_{ni}\} \\
\dot{X}_{G_i} & = V_{a_i} cos\gamma_{a_i} cos\chi_{a_i} \\
\dot{Y}_{G_i} & = V_{a_i} cos\gamma_{a_i} sin\chi_{a_i} \\
\dot{Z}_{G_i} & = -V_{a_i} sin\gamma_{a_i} \\
\dot{\phi}_i & = p_i + q_i sin\phi_i tan\theta_i + r_i cos\phi_i tan\theta_i \\
\dot{\theta}_i & = q_i cos\phi_i - r_i sin\phi_i \\
\dot{\psi}_i & = \frac{sin\phi_i}{cos\theta_i}q_i + \frac{cos\phi_i}{cos\theta_i}r_i \\
\dot{m}_i & = -2.01 \times 10^{-5}\frac{(\Phi - \mu - \frac{K}{\eta_c})\sqrt{\Theta}}{\sqrt{5\eta_n(1+\eta_{tf}\lambda)}\sqrt{G+0.2M^2\frac{\eta_d}{\eta_{tf}}\lambda - (1-\lambda)M}}\frac{1}{2}\rho S V_{ai}^2 C_D
\end{cases}
\tag{7}
$$

By the combination of this system with the aircraft control, one has the two-aircraft dynamic flight model as shown in (6). The state vector is

$$
\begin{aligned}
y_i(t) & : [t_0, t_f] \longrightarrow \mathbf{R^{12}} \\
y_i(t) & = (\alpha_{ai}(t), \theta_{ai}(t), \psi_{ai}(t), \phi_{ai}(t), V_{a_i}(t), X_{G_i}(t), Y_{G_i}(t), Z_{G_i}(t), p_i(t), \\
& \quad q_i(t), r_i(t), m_i(t))
\end{aligned}
\tag{8}
$$

This will be added to the cost function and constraint function for the aircraft optimal control problem as shown in the following paragraphs.

The objective function model. In this paper, the considered cost function is the Sound Exposure Level 'SEL'[1, 22, 28]:

$$
SEL = 10log\left[\frac{1}{t_o}\int_{t'} 10^{0.1L_{A1,dt}(t)}dt\right]
\tag{9}
$$

where t_o is the time reference taken equal to 1 s and t' the noise event interval. $[t_{10}, t_{1f}]$ and $[t_{20}, t_{2f}]$ are the respective approach intervals for the first and the

second aircraft, the objective function is calculated as:

$$
\begin{aligned}
SEL_1 &= 10log\left[\frac{1}{t_o}\int_{t_{10}}^{t_{20}}10^{0.1L_{A1,dt}(t)}dt\right], t \in [t_{10}, t_{20}]\\
SEL_{12} &= SEL_{11} \oplus SEL_{21}\\
&= 10\log[\frac{1}{t_o}\int_{t_{20}}^{t_{1f}}10^{0.1L_{A1,dt}(t)}dt + \frac{1}{t_o}\int_{t_{20}}^{t_{1f}}10^{0.1L_{A2,dt}(t)}dt], t \in [t_{20}, t_{1f}]\\
SEL_2 &= 10\log\left[\frac{1}{t_o}\int_{t_{1f}}^{t_{2f}}10^{0.1L_{A2,dt}(t)}dt\right], t \in [t_{1f}, t_{2f}]\\
SEL_G &= \frac{(t_{20}-t_{10})SEL_1 \oplus (t_{1f}-t_{20})SEL_{12} \oplus (t_{2f}-t_{1f})SEL_2}{t_{2f}-t_{10}}\\
&= 10\log\{\frac{1}{t_{2f}-t_{10}}[(t_{20}-t_{10})\int_{t_{10}}^{t_{20}}10^{0.1L_{A1}(t)}dt\\
&+(t_{1f}-t_{20})\int_{t_{20}}^{t_{1f}}10^{0.1L_{A1}(t)}dt + (t_{1f}-t_{20})\int_{t_{20}}^{t_{1f}}10^{0.1L_{A2}(t)}dt\\
&+(t_{2f}-t_{1f})\int_{t_{1f}}^{t_{2f}}10^{0.1L_{A2}(t)}dt,]\}, t \in [t_{10}, t_{2f}]
\end{aligned}
$$

(10)

where SEL_G is the cumulated two-aircraft noise and the operator $\oplus$ means the acoustic adding. Expressions $L_{A1}(t), L_{A2}(t)$ are equivalent and reflect the aircraft jet noise given by the formula [1, 20]:

$$
\begin{aligned}
L_{A1}(t) &= 141 + 10\log\left(\frac{\rho_1}{\rho}\right)^w + 10\log\left(\frac{V_e}{c}\right)^{7.5} + 10\log s_1\\
&+3\log\left(\frac{2s_1}{\pi d_1^2}+0.5\right) + 5\log\frac{\tau_1}{\tau_2}\\
&+10\log\left[\left(1-\frac{v_2}{v_1}\right)^{me} + 1.2\frac{\left(1+\frac{s_2 v_2^2}{s_1 v_1^2}\right)^4}{\left(1+\frac{s_2}{s_1}\right)^3}\right]\\
&-20\log R + \Delta V + 10\log\left[\left(\frac{\rho}{\rho_{ISA}}\right)^2\left(\frac{c}{c_{ISA}}\right)^4\right]
\end{aligned}
$$

where v_1 is the jet speed at the entrance of the nozzle, v_2 the jet speed at the nozzle exit, τ_1 the inlet temperature of the nozzle, τ_2 the temperature at the nozzle exit, ρ the density of air, ρ_1 the atmospheric density at the entrance of the nozzle, ρ_{ISA} the atmospheric density at ground, s_1 the entrance area of the nozzle hydraulic engine, s_2 the emitting surface of the nozzle hydraulic engine, d_1 the inlet diameter of the nozzle hydraulic engine, $V_e = v_1[1 - (V/v_1)\cos(\alpha_p)]^{2/3}$ the effective speed (α_p is the angle between the axis of the motor and the axis of the aircraft), R the source observer distance, w the exponent variable defined by: $w = \frac{3(V_e/c)^{3.5}}{0.6 + (V_e/c)^{3.5}} - 1$, c the sound velocity (m/s), m the exhibiting variable depending on the type of aircraft: $me = 1.1\sqrt{\frac{s_2}{s_1}}$; $\frac{s_2}{s_1} < 29.7$, $me = 6.0$; $\frac{s_2}{s_1} \geq 29.7$, the term $\Delta V = -15log(C_D(M_c, \theta)) - 10log(1 - Mcos\theta)$, means the Doppler convection

when $C_D(M_c, \theta) = [(1 + M_c cos\theta)^2 + 0.04M_c^2]$, M the aircraft Mac Number, M_c the convection Mac Number: $M_c = 0.62(v_1 - V cos(\alpha_p))/c$, θ is the Beam angle.

Formula above leads to the objective function $J_{G12}(y(t), u(t), i = 1, 2) = \int_{t'} g(y(t), u(t), t, i = 1, 2)dt$.

Constraints. The considered constraints concern aircraft flight speeds and altitudes, flight angles and control positions, energy constraint, aircraft separation, flight velocities of aircraft relative to the earth and the aircraft mass:

1. The vertical separation given by $Z_{G12} = Z_{G2} - Z_{G1}$ where Z_{G1}, Z_{G2} are respectively the altitude of the first and the second aircraft and Z_{G12} the altitude separation.

2. The horizontal separation $X_{G12} = X_{G1} - X_{G2}$ [13, 14, 38] where X_{G1}, X_{G2} are horizontal positions of the first and the second aircraft and their separation distance.

3. The aircraft speed V_{a_i} must be bounded as follows $1.3V_s \le V_{a_i} \le V_{if}$ where V_s is the stall speed, V_{if} is the maximum speed and $V_{io} = 1.3V_s$ the minimum speed of the aircraft A_i [15, 36], the roll velocity of the aircraft relative to the earth $p_i \in [p_{i0}, p_{if}]$, the pitch velocity of the aircraft relative to the earth $q_i \in [q_{i0}, q_{if}]$ and the yaw velocity of the aircraft relative to the earth $r_i \in [r_{i0}, r_{if}]$.

4. On the approach, the ICAO standards and aircraft manufacturers require flight angle evolution as follows: attack angle $\alpha_{a_i} \in [\alpha_{io}, \alpha_{if}]$, the inclination angle $\theta_i \in [\theta_{i0}, \theta_{if}]$ and the roll angle $\phi_i \in [\phi_{io}, \phi_{if}]$.

5. The aircraft control $\delta(t) = (\delta_{l_i}(t), \delta_{m_i(t)}, \delta_{n_i}(t), \delta_{x_i}(t))$ keeps still between the position δ_{li0} and δ_{lif} for the roll control, δ_{mi0} and δ_{mif} for the pitch control, δ_{ni0} and δ_{nif} for the yaw control and δ_{xi0} and δ_{xif} for the thrust.

6. The mass m_i of the aircraft A_i is variable: $m_{i0} < m_i < m_{if}, i = 1, 2$. This constraint results in energy consumption of the aircraft [8, 24].

On the whole, the constraints come together under the relationship:

$$
\begin{aligned}
k_{1i}(y_i(t), u_i(t)) &\le 0 \\
k_{2i}(y_i(t), u_i(t)) &\ge 0
\end{aligned}
\tag{11}
$$

where

$$k(t) \quad : \mathbf{R^{12}} \times \mathbf{R^4} \longrightarrow \mathbf{R^{16}},$$
$$(y_i(t), u_i(t)) \longrightarrow k_i(y_i(t), u_i(t))$$
$$k_{1i}(y_i(t), u_i(t)) = (\alpha_i(t) - \alpha_{if}, \theta_i(t) - \theta_{if}, \psi_i(t) - \psi_{if}, \phi_i(t) - \phi_{if},$$
$$V_{a_i}(t) - V_{aif}, X_{G_i}(t) - X_{Gif}, Y_{G_i}(t) - Y_{Gif}, Z_{G_i}(t) - Z_{Gif},$$
$$p_i(t) - p_{if}, q_i(t) - q_{if}, r_i(t) - r_{if}, \delta_{l_i}(t) - \delta_{l_if}, \delta_{m_i}(t) - \delta_{mif},$$
$$\delta_{n_i}(t) - \delta_{nif}, \delta_{x_i}(t) - \delta_{xif}, m_i(t) - m_{if})$$
$$k_{2i}(y_i(t), u_i(t)) = (\alpha_i(t) - \alpha_{i0}, \theta_i(t) - \theta_{i0}, \psi_i(t) - \psi_{i0}, \phi_i(t) - \phi_{i0},$$
$$V_{a_i}(t) - V_{ai0}, X_{G_i}(t) - X_{Gi0}, Y_{G_i}(t) - Y_{Gi0}, Z_{G_i}(t) - Z_{Gi0},$$
$$p_i(t) - p_{i0}, q_i(t) - q_{i0}, r_i(t) - r_{i0}, \delta_{l_i}(t) - \delta_{l_i0}, \delta_{m_i}(t) - \delta_{mi0},$$
$$\delta_{n_i}(t) - \delta_{ni0}, \delta_{x_i}(t) - \delta_{xi0}, m_i(t) - m_{i0}).$$

The following values reflect the digital applications considered for the two-aircraft [1, 7, 8, 36].

Table of limit digital values for the two-aircraft in approach phase		
Constraint denomination	maximum value	minimum value
The Aircraft speed	$V_{a1f} = V_{a2f} = 200 \ m/s$	$V_{a10} = V_{a20} = 73.45 \ m/s$
The A1 Aircraft altitude	$Z_{G1f} = 35 \times 10^2 \ m$	$Z_{G10} = 0 \ m$
The A2 Aircraft altitude	$Z_{G2f} = 41 \times 10^2 \ m$	$Z_{G20} = 0 \ m$
The aircraft roll control	$\delta_{l1f} = \delta_{l2f} = 0.0174$	$\delta_{l10} = \delta_{l20} = -0.0174$
The pitch control	$\delta_{m1f} = \delta_{m2f} = 0.087$	$\delta_{m10} = \delta_{m20} = 0$
The yaw control	$\delta_{n1f} = \delta_{n2f} = 0.314$	$\delta_{n10} = \delta_{n20} = -0.035$
The thrust control	$\delta_{x1f} = \delta_{x2f} = 0.6$	$\delta_{x10} = \delta_{x20} = 0.2$
The attack angle	$\alpha_{a1f} = \alpha_{a2f} = 12°$	$\alpha_{a10} = \alpha_{a20} = 2°$
The inclination angle	$\theta_{a1f} = \theta_{a2f} = 7°$	$\theta_{a10} = \theta_{a20} = -7°$
The air-path inclination angle	$\gamma_{a1f} = \gamma_{a2f} = 0°$	$\gamma_{a10} = \gamma_{a20} = -5°$
The aerodynamic bank angle	$\mu_{a1f} = \mu_{a2f} = 3°$	$\mu_{a10} = \mu_{a20} = -2°$
The air-path azimuth angle	$\chi_{a1f} = \chi_{a2f} = 5°$	$\chi_{a10} = \chi_{a20} = -5°$
The roll angle	$\phi_{a1f} = \phi_{a2f} = 1°$	$\phi_{a10} = \phi_{a20} = -1°$
The cup	$\psi_{a1f} = \psi_{a2f} = 3°$	$\psi_{a10} = \psi_{a20} = -3°$
The limits of time	$t_{1f} = 600 \ s, t_{2f} = 645 \ s$	$t_{10} = 0 \ s, \ t_{20} = 45 \ s$
The mass of the A1 Aircraft	$m_{10} \simeq 1.1 \times 10^5 \ kg,$	$m_{1f} \simeq 1.09055 \times 10^5 \ kg,$
The mass of the A2 Aircraft	$m_{20} \simeq 1.10071 \times 10^5 \ kg$	$m_{2f} \simeq 1.09126 \times 10^5 \ kg$
The A300 inertia moments [8]	$A = 5.555 \times 10^6 \ kg \ m^2$	$B = 9.72 \times 10^6 \ kg \ m^2$
	$C = 14.51 \times 10^6 \ kg \ m^2$	$E = -3.3 \times 10^4 \ kg \ m^2$
The Aircraft vertical separation	$Z_{12} = 2 \times 10^3 \ ft \simeq 6 \times 10^2 \ m$	
The Aircraft longitudinal separation	$X_{G12} = 5 \ NM \simeq 9 \times 10^3 \ m$	
The Aircraft roll velocity relative to the earth	$p_{1f} = p_{2f} = 1° s^{-1}$	$p_{10} = p_{20} = -1° s^{-1}$
The Aircraft pitch velocity relative to the earth	$q_{1f} = q_{2f} = 3.6° s^{-1}$	$q_{10} = q_{20} = 3° s^{-1}$
The Aircraft yaw velocity relative to the earth	$r_{1f} = r_{2f} = 12° s^{-1}$	$r_{10} = r_{20} = -12° s^{-1}$

Table 1.

The two-aircraft acoustic optimal control problem. The combination of the aircraft dynamic equation (3) and (7), the aircraft objective function from equations (10) and the the aircraft flight constraints (11), the two-aircraft

acoustic optimal control problem is given as follows:

$$
\begin{cases}
\min_{(y,u)\in\mathbf{Y}\times\mathbf{U}} J_{G12}(y(t),u(t)) = \int_{t10}^{t_{1f}} g_1(y_1(t),u_1(t),t)dt + \\
\int_{t20}^{t_{1f}} g_{12}(y_1(t),u_1(t),y_2(t),u_2(t),t)dt + \int_{t20}^{t_{2f}} g_2(y_2(t),u_2(t),t)dt + \phi(y(t_f)) \\
\dot{y}(t) = f(u(t),y(t)), u(t) = (u_1(t),u_2(t)), y(t) = (y_1(t),y_2(t)), \\
\forall t \in [t_{10},t_{2f}], t_{10} = 0, y(0) = y_0, u(0) = u_0 \\
k_{1i}(y_i(t),u_i(t)) \leq 0 \\
k_{2i}(y_i(t),u_i(t)) \geq 0
\end{cases}
$$

(12)

where g_{12} shows the aircraft coupling noise function and J_{G12} is the SEL of the two A300-aircraft.

3   The numerical processing

The problem as defined in the relation (12) is an optimal control problem with instantaneous constraints. We aim to solve this problem with the Trust Region Sequential Quadratic Programming method. Applying SQP methods[10, 32] , we write the system (12) as:

$$
\begin{cases}
\min J_{G12}(x), x = (y(t),u(t)) \\
\dot{y} = f(x) \\
n_j(x) \leq 0, j \in \Xi \\
n_j(x) \geq 0, j \in \Gamma
\end{cases}
$$

(13)

where the expressions Ξ and Γ are the sets of equality and inequality indices. The function $J_{G12}(x), f(x), n(x)$ must be twice continuously differentiable. The Lagrangian of the system (13) is defined by the function $L(x,\lambda) = J_{GP12}(x) + \lambda^T[b(\dot{y},x) + n(x)]$ where the vector λ is the Lagrange multiplier and $b(\dot{y},x) = \dot{y} - f(x) = 0$. Considering the feasible points of (12), one transforms the system (13) into a quadratic problem. A SQP method solves a succession of quadratic problems. The mathematical formulation of sub-problems obtained at the k-th step Δx_k is the following:

$$
\begin{cases}
\min_{\Delta x_k}[K_{G12}(x_k)] = \nabla^T J_{G12}(x_k)\Delta x_k + \frac{1}{2}(\Delta x_k)^T H_k \Delta x_k \\
\nabla^T b(\dot{y}_k,x_k)\Delta x_k + b(\dot{y}_k,x_k) = 0 \\
\nabla^T n_{\Xi}(x_k)\Delta x_k + n_{\Xi}(x_k) \leq 0 \\
\nabla^T n_{\Gamma}(x_k)\Delta x_k + n_{\Gamma}(x_k) \geq 0
\end{cases}
$$

(14)

The vector Δx_k is a primal-dual descent direction, $H_k = \nabla^2 L(x_k,\lambda_k)$ is the Hessian matrix of Lagrangian L from system (13) and $K_{G12}(x_k)$ the quadratic model. The estimation of gradients is, in principle, calculated by finite differences or the calculation of the adjoint systems for problems with many parameters and finally by the sensitivity analysis. This last technique is very

effective in the case of a large number of variables with few parameters [3, 11]. The SQP method is a qualified local method. Its convergence is quadratic if the first iterate is close to a solution $\tilde{y}$ satisfying the sufficient optimality conditions [9, 18, 21]. This algorithm above must be transformed because the two-Aircraft problem is non-convex. For improving the robustness and global convergence behavior of this SQP algorithm, it must be added with the trust radius of this form:

$$||D\Delta x_k||_p \leq \Delta, p \in [1, \infty] \tag{15}$$

where D is uniformly bounded. The relations (14) and (15) form a quadratic program when $p = \infty$. So, the trust-region constraint is restated as $-\Delta e \leq Dx \leq \Delta e, e = (1, 1, 1, ..., 1)^T$. If $p = 2$, one has the quadratic constraint $\Delta x_k^T D^T D \Delta x_k \leq \Delta^2$. In the following, we develop the convergence theory for any choice of p just to show the equivalence between the $||.||_p$ and $||.||_2$. By the combination of some relation of (13) and the relation (14), all the components of the step are controlled by the trust region. The two-aircraft problem takes the following form

$$\begin{cases} \min_{\Delta x_k}[K_{G12}(x_k)] = \nabla^T J_{G12}(x_k)\Delta x_k + \frac{1}{2}(\Delta x_k)^T H_k \Delta x_k \\ \nabla^T b(\dot{y}_k, x_k)\Delta x_k + b(\dot{y}_k, x_k) = 0 \\ \nabla^T n_\Xi(x_k)\Delta x_k + n_\Xi(x_k) \leq 0 \\ \nabla^T n_\Gamma(x_k)\Delta x_k + n_\Gamma(x_k) \geq 0 \\ ||D\Delta x_k||_p \leq \Delta, p \in [1, \infty] \end{cases} \tag{16}$$

In some situations, all of the components of the step are not controlled by the trust region because of some hypotheses on D. There is an other alternative which allows the practical SQP methods by using the merit function or the penalty function to measure the worth of each point x.

Several approaches like Byrd-Omojokun and Vardi approaches exist to solve the system (13) [42]. It can also be solved with the KNITRO, the SNOPT and other methods [34]. In the latter case, we have an ordinary differential system of non-linear and non-convex equations. The uniqueness of the solution of the quadratic sub-problem is not guaranteed. It therefore combines the algorithm with a merit function for judging the quality of the displacement. The merit function can therefore offer a way to measure all progress of iterations to the optimum while weighing the importance of constraints on the objective function. It is chosen in l_2 norm particularly the increased Lagrangian L_I because of its smooth character. So, in the equation above, one replaces L by L_I. Thus, this transforms the SQP algorithm in sequential quadratic programming with trust region globalization 'TRSQP'. Its principle is that each new iteration must decrease the merit function of the problem for an eligible trust radius. Otherwise, we reduce the trust radius Δx_K for computing the new displacement. A descent direction is acceptable if its reduction is emotionally positive. The advantages of the method are that the merit function will circumvent the

non-convexity of the problem. This approach shows that only one point is sufficient to start the whole iterative process [19, 25, 31].

Meanwhile, we use an algorithm called feasibility perturbed SQP in which all iterates x_k are feasible and the merit function is the cost function. Let us consider the perturbation $\tilde{\Delta x_k}$ of the step Δx_k such that

1. The relation

$$x + \tilde{\Delta x_k} \in \mathbf{F} \tag{17}$$

   where $\mathbf{F}$ is the set of feasible points for (12),

2. The asymptotic exactness relation

$$||\Delta x - \tilde{\Delta x_k}||_2 \leq \phi(||\Delta x_k||_2)||\Delta x_k||_2 \tag{18}$$

   is satisfied where $\phi : \mathbb{R}^+ \longrightarrow \mathbb{R}^+$ with $\phi(0) = 0$.

These two conditions are used to prove the convergence of the algorithm and the effectiveness of this method. The advantages gained by maintaining feasible iterates for this method are:

- The trust region restriction (15) is added to the SQP problem (14) without concern that it will yield an infeasible subproblem.

- The objective function J_{G12} is itself used as a merit function in deciding whether to take a step.

- If the algorithm is terminated early, we will be able to use the latest iterate x_k as a feasible suboptimal point, which in many applications is far preferable to an infeasible suboptimum.

Here are some considerations that are needed for the KKT optimality conditions.

- *An inequality constraint n_j is active at point $\tilde{x} = (y^*, u^*)$ if $n_j(\tilde{x}) = 0$. $\Gamma(\tilde{x}) = \Gamma^*$ is the set of indices j corresponding to active constraints in $\tilde{x}$,*

$$\begin{aligned} \Gamma_*^+ &= \{j \in \Gamma_* | (\lambda_\Gamma^*)_j > 0\} \\ \Gamma_*^0 &= \{j \in \Gamma_* | (\lambda_\Gamma^*)_j = 0\} \end{aligned} \tag{19}$$

  where the constraints of index Γ_*^+ are highly active and those of Γ_*^0 weakly active.

- *An element $\tilde{x} \in \Gamma^*$ verifies the condition of qualifying for the constraints n if the gradients of active constraint $\nabla n_\Xi(\tilde{x}), \nabla n_\Gamma(\tilde{x})$ are linearly independent. This means that the Jacobian matrix of active constraints in $\tilde{x}$ is full.*

- *An element $\tilde{x} \in \Gamma^*$ satisfies the qualification condition of Mangasarian-Fromowitz for constraints n in $\tilde{x}$ if there exists a direction d such that*

$$\nabla n_\Xi(\tilde{x})^T d = 0 \nabla n_j(\tilde{x})^T d < 0 \forall j \in \Gamma(\tilde{x}) \tag{20}$$

  where the gradients $\{\nabla n(\tilde{x})\}$ are linearly independent.

The Karush-Kuhn-Tucker optimality conditions are obtained by considering that J, n functions of C^1 class and $\tilde{x}$ a solution of the problem (12) which satisfies a constraints qualification condition. So,there exists λ^* such that:

$$\nabla_y L(\tilde{x}, \lambda^*) = 0, n_\Xi(\tilde{x}) = 0, n_\Gamma(\tilde{x}) \leq 0, \lambda_\Gamma^* \geq 0, \lambda_\Gamma^* n_\Gamma(\tilde{x}) = 0 \tag{21}$$

These equations are called the conditions of Karush-Kuhn-Tucker(KKT). The first equation reflects the optimality, the second and third the feasibility conditions. The others reflect the additional conditions and Lagrange multipliers corresponding to inactive constraints $nj(\tilde{x})$ are zero. The couple $(\tilde{x}, \lambda^*)$ such that the KKT conditions are satisfied is called primal-dual solution of (19). So, $\tilde{x}$ is called a stationary point.

For the necessary optimality conditions of second order [5], taking $\tilde{x}$ a local solution of (19) and satisfying a qualification condition, then there exist multipliers (λ^*) such that the KKT conditions are verified . So we have $\nabla^2_{xx} L(\tilde{x}, \lambda^*).d.d > 0 \forall h \in \mathbf{C}_*$ where $\mathbf{C}_*$ is a critical cone defined by $C_* = \{h \in \mathbf{Y} \times \mathbf{U} : \nabla n_j(\tilde{x}).h = 0 \ \forall j \in \Xi \cup \Gamma_*^+, \nabla n_j(\tilde{x}).h \leq 0 \forall j \in \Gamma_*^0\}$. The elements of C^* are called critical directions.

For the sufficient optimality conditions of second order [5], suppose that there exists (λ^*) which satisfy the KKT conditions and such that $\nabla^2_{xx} L(\tilde{x}, \lambda^*).d.d > 0 \forall h \in \mathbf{C}_* \backslash \{0\}$. So $\tilde{x}$ is a local minimum of(12).

4 The TRSQP algorithm and convergence analysis

Assume that for a given SQP step Δx_k and its perturbation $\tilde{\Delta x_k}$, the ratio to predict decrease is

$$r_k = \frac{J_{G12}(x_k) - J_{G12}(x_k + \tilde{\Delta x_k})}{-K_{G12}(\tilde{\Delta x_k})} \tag{22}$$

The two-aircraft acoustic optimal control TRSQP algorithm is written as:

1. Let x_0 a given starting point, $\overline{\Delta} \geq 1$ the trust region upper bound, $\Delta_0 \in (0, \overline{\Delta})$ an initial radius, $\epsilon \in [\epsilon_0, \epsilon_f)$ and $p \in [1, \infty]$

2. Calculate Δx_k by solving the system

$$\begin{cases} \min_{\Delta x_k}[K_{G12}(x_k)] = \nabla^T J_{G12}(x_k)\Delta x_k + \frac{1}{2}(\Delta x_k)^T H_k \Delta x_k \\ \nabla^T b(\dot{y}_k, x_k)\Delta x_k + b(\dot{y}_k, x_k) = 0 \\ \nabla^T n_\Xi(x_k)\Delta x_k + n_\Xi(x_k) \leq 0 \\ \nabla^T n_\Gamma(x_k)\Delta x_k + n_\Gamma(x_k) \geq 0 \\ ||D\Delta x_k||_p \leq \Delta, p \in [1, \infty] \end{cases}$$

Seek also $\tilde{\Delta x}_k$ by using the system

$$x + \tilde{\Delta x}_k \in \mathbf{F}$$
$$||\Delta x - \tilde{\Delta x}_k||_2 \leq \phi(||\Delta x_k||_2)||\Delta x_k||_2$$

3. If no such for the perturbed counterpart $\tilde{\Delta x}_k$ is found, the following affectations are considered.

$$\Delta x_{k+1} \leftarrow (\tfrac{1}{2})||D_k \Delta x_k||_p$$
$$x_{k+1} \leftarrow x_k; D_{k+1} \leftarrow D_k;$$

4. Otherwise, calculate $r_k = \frac{J_{G12}(x_k) - J_{G12}(x_k + \tilde{\Delta x}_k)}{-K_{G12}(\tilde{\Delta x}_k)}$;
   if $r_k \leq \epsilon_f, \Delta_{k+1} \leftarrow (\tfrac{1}{2})||D_k \Delta x_k||_p$;
   else if $r_k > a_0 \times \epsilon_0$ and $||D_k \Delta x_k||_p = \Delta_k$
   $\Delta_{k+1} \leftarrow min(2\Delta_k, \Delta)$;
   else $\Delta_{k+1} \leftarrow \Delta_k$;

5. If $r_k > \epsilon$ $x_{k+1} \leftarrow x_k + \tilde{\Delta x}_k$; Choose the new matrix D_{k+1};
   else $x_{k+1} \leftarrow x_k; D_{k+1} \leftarrow D_k$;

6. end.

At each major iteration a positive definite quasi-Newton approximation of the Hessian of the Lagrangian function, H, is calculated using the BFGS method, where $\lambda_i, i = 1, ..., m$, is an estimate of the Lagrange multipliers.

$$H_{k+1} = H_k + \frac{q_k q_k^T}{q_k^T s_k} - \frac{H_k^T s_k^T s_k H_k}{s_k^T H_k s_k}$$

where

$$\begin{aligned} s_k &= x_{k+1} - x_k, \\ q_k &= (\nabla J_{G12}(x_{k+1} + \sum_{j=1}^n \lambda_j.\nabla n(x_{k+1}) + b(x_{k+1})) \\ &\quad -(\nabla J_{G12}(x_k + \sum_{j=1}^n \lambda_j.\nabla n(x_k) + b(x_k)) \end{aligned}$$

A positive definite Hessian is maintained providing $q_k^T s_k$ is positive at each update and that H is initialized with a positive definite matrix. This algorithm

is implemented by AMPL language programming and the KNITRO solver [33].

Analysis of the algorithm and its convergence.   Let us define the set $\mathbf{F_0}$ as follows: $\mathbf{F_0} = \{x | \nabla^T b(\dot{y}, x)\Delta x + b(\dot{y}, x) = 0, \nabla^T n_\Xi(x)\Delta x + n_\Xi(x) = 0, \nabla^T n_\Gamma(x)\Delta x + n_\Gamma(x) \geq 0, J_{G12}(x) \leq J_{G12}(x_0)\} \in \mathbf{F}$ The trust-region bound $||D\Delta x_k||_p \leq \Delta, p \in [1, \infty]$ specifies the following assumption.

1. There exists a constant β such that for all points $x \in \mathbf{F_0}$ and all matrix D used in the algorithm, we have for any Δx satisfying the following equations

$$\nabla^T b(\dot{y}, x)\Delta x + b(\dot{y}, x) = 0,$$
$$\nabla^T n_\Xi(x)\Delta x + n_\Xi(x) = 0,$$
$$\nabla^T n_\Gamma(x)\Delta x + n_\Gamma(x) \geq 0.$$

   that

$$\beta^{-1}||\Delta x||_2 \leq ||D\Delta x||_p \leq \beta||\Delta x||_2 \tag{23}$$

2. The level set $\mathbf{F_0}$ is bounded and the functions J_{G12}, b, η are twice continuously differentiable in an open neighborhood $\mathbf{M(F_0)}$ of this set.

Under certain assumptions as shown in [30], this algorithm is well defined.

In this paragraph, one wants to prove that the algorithm has a convergence to stationary point of (13). If we consider that all assumptions hold for each feasible point $\tilde{x}$ for (12), the Mangasarian-Fromowitz are satisfied for constraints. After all, the KKT optimality conditions are specified and that shows that there is at least a local convergence. With other added conditions as shown in [30], the global convergence is held.

5   Numerical Results

The observation points are taken on the ground under the flight path and are independent of each other. Numerical processing is implemented by AMPL and KNITRO solver. KNITRO output optimality conditions for the obtained solution is achieved as follow:
Multistart stopping, found local optimal solution.

MULTISTART: Best locally optimal point is returned.
EXIT: Locally optimal solution found.
Final Statistics:
Final objective value = 4.91134561926630e+01
Final feasibility error (abs / rel) = 5.79e-09 / 1.96e-10
Final optimality error (abs / rel) = 2.58e-07 / 2.58e-07

Number of iterations = 72
Number of CG iterations = 3
Number of function evaluations = 85
Number of gradient evaluations = 73
Number of Hessian evaluations = 72
Total program time (secs) = 258.19754 (258.104 CPU time)
Time spent in evaluations (secs) = 240.00644

The observation positions are:
$(-20000\ m, -20000\ m, 0\ m), (-19800\ m, -19800\ m, 0\ m), ..., (0\ m, 0\ m, 0\ m)$,
for a space step of $200\ m$ for x and y. The touch point on the ground is
$(0\ m, 0\ m, 0\ m)$ while the temporal separation of aircraft is $90\ s$. At each
point, it is a vector of N noise levels as shown in the discretization process. It
is very important to consider the maximum value among the N values, which
value corresponds to the shortest distance between the noise source and the
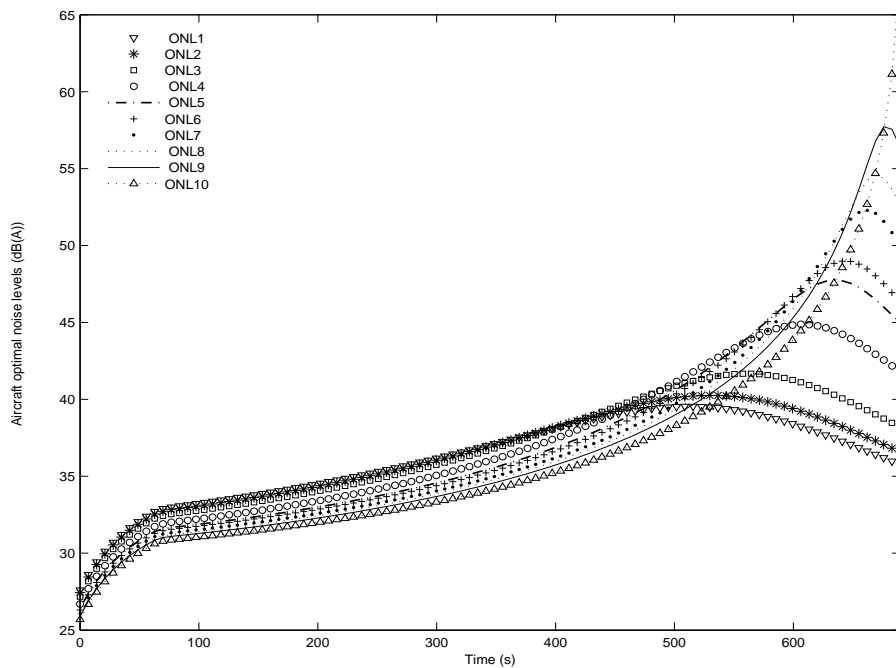observation point.

Figure 1: Aircraft noise at the indicated reception point

Figure 1 shows the noise levels when the optimization is applied and the
solutions obtained. The observation positions are $(-20000\ m, -20000\ m, 0\ m)$
for ONL_1 , $(-19800\ m, -19800\ m, 0\ m)$ for ONL_1,..., $(-200\ m, -200\ m, 0\ m)$

for ONL_{10}. In this figure, the legend ONL means optimal noise level. As specified, noise level increases (till 550 sec) and is maximum when the observation point lies below the aircraft. Noise levels decrease gradually as the aircraft moves away from the observation point. This is confirmed by Khardi analysis [26]. By comparison, this result is also close to standard values of jet noise on approach as shown by Harvey [2, 23]. To conclude, numerical calculations carried out in this paper are efficient and fitted with experimental and theoretical researches related to acoustical developments.
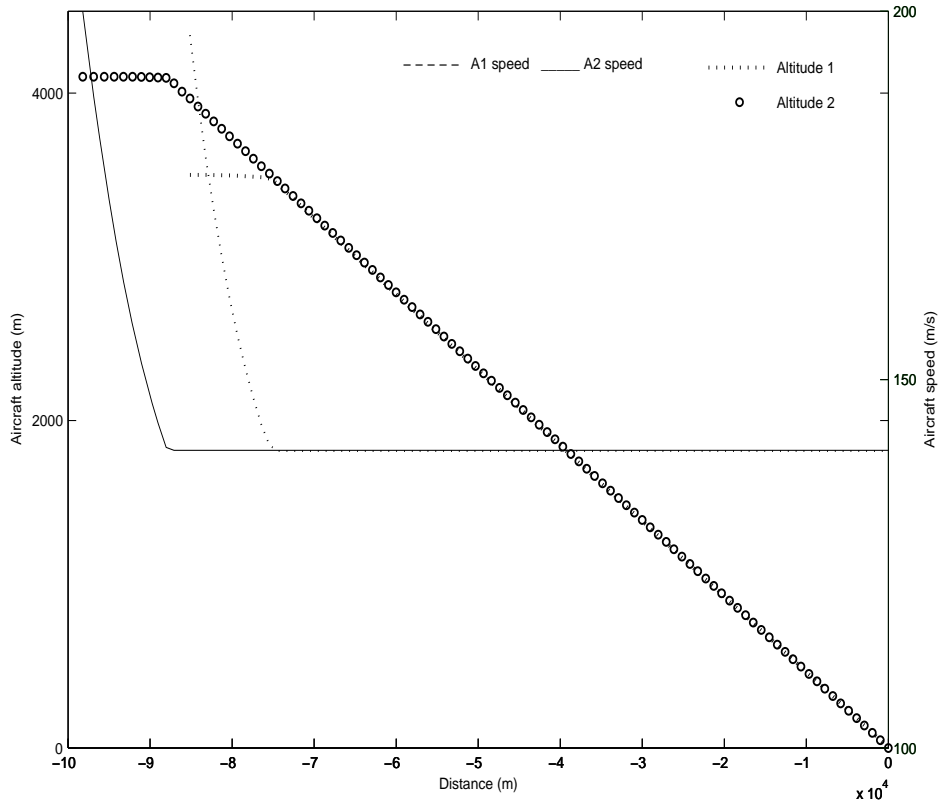

Figure 2: Aircraft optimal flight paths and speeds

Figure 2 shows the trajectories which reflect a path in one level flight followed by a continuous descent till the aircraft touch point. The aircrafts' landing procedures are sufficiently separated. It is obvious that each aircraft follows its optimal trajectory when considering the separation distance. Constraints on speeds described in the previous table are considered, allowing a subsequent landing on the same track. Thus, as recommended by ICAO, the security conditions are met and flight procedures are good as shown by the

presented results. The maximum altitudes considered are 3500 m and 4100 m for the first and the second aircraft. The duration approach is 600 s for the first aircraft and 690 s for the second. This figure shows that after some time, we have obtained the same optimal trajectory for the two-aircraft even the procedures are different. This shows the aircraft trajectory resulting from the two trajectories combination. This figure also shows aircraft speed evolution during landing. For the first, the aircraft speed decreases from 200 m/s to 140 m/s and keeps a constant position till the end of the aircraft landing. This evolution remains the same for the speed of the second aircraft.
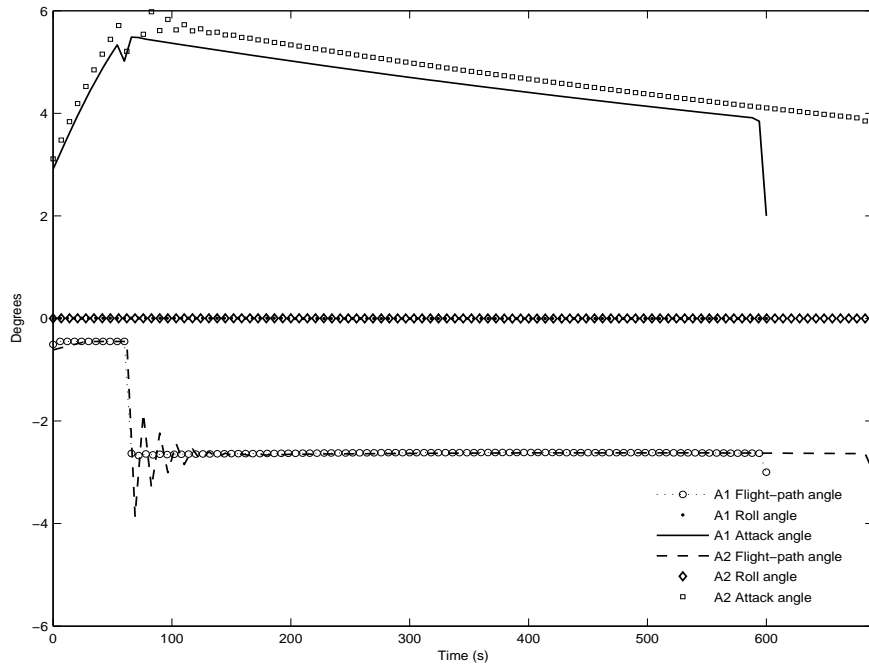

Figure 3: Flight-path angles of the aircraft

Figure 3 shows the aircraft angles versus time as recommended by ICAO during aircraft landing. As specified by this figure, the aircraft roll angles oscillate around zero, the flight-path angles are negative and keep the recommended position for aircraft landing procedures. This is the same for the attack angles. Angular variations confirmed the aircraft aerodynamic stability and the flight safety.
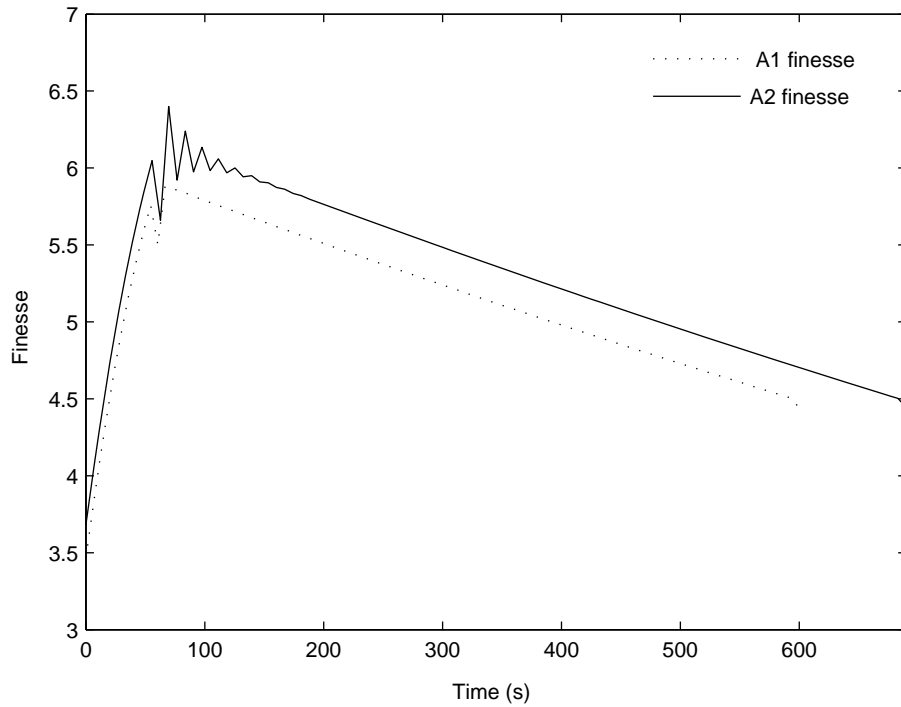
Figure 4: Aircraft finesse

Figure 4 shows the finesse for the two aircraft. The behavior of the finesse confirms the stability of the aircraft flight. That reflects the flight procedures characteristic as shown by figures 2, 3 and 4. Processing calculation provided that the aircraft throttle position is kept constant (0.6) during the landing procedures. The two-aircraft roll velocity p_1, p_2, pitch velocity q_1, q_2 and yaw velocity r_1, r_2, both related to earth frame, are obtained and they have a constant behavior.

6   Conclusion

We have developed a mathematical model in the case of two approaching aircraft landing in succession on the same track. An algorithm for solving the optimal control model has been developed. Theoretical considerations and practices of the feasible TRSQP algorithm are used by KNITRO for the establishment of a non-linear program, implementing the considered problem. The algorithm minimizes a sequence of merit function using a sub-problem of the quadratic problem at each step for all active constraints to generate a search trust direction for all primal and dual variables. An optimal solution to the

discretized problem is found through a local convergence. The results show a reduction of noise at reception points during the approach of the two-aircraft. The obtained trajectories exhibit optimal characteristics and are acoustically effective. Some added conditions are necessary to prove the global convergence of the considered algorithm. We found that the aircraft optimal trajectories coincide for a large portion of the flight as soon as the continuous descent is initiated. Further researches are needed to complete the problem processing.

References

[1] L. Abdallah, Minimisation des bruits des avions commerciaux sous contraintes physiques et aérodynamique, *Thèse de Mathématiques Appliquées de l'UCBL I,* Septembre 2007.

[2] L. Abdallah, M. Haddou and S. Khardi, Optimization of operational aircraft parameters reducing noise emission, *Applied Mathematical Sciences,* **4, 11** (2010), 515-535.

[3] S. Avdoshin, A. Hait, J-M. Le Lann, A. Mitsiouk and S. Negny, Optimisation des Systèmes dynamiques hybrides, Application en génie industriel à l'élaboration des scenarios, *Institut National Polytechnique de Toulouse,* 2003

[4] N. Barriety and J-P. Jung, La voie de la science, Des outils pour optimiser la conception des avions en phase d'approche, *horizon Onera Midi-Pyrenees,* Toulouse December 2008.

[5] M. Bergounioux, Optimisation et Controle des systèmes linéaires, Cours et exercices corrigés, Dunod, 2002.

[6] K. Blin,Stochastic conflict detection for air traffic management, *Eurocontrol Experimental centre Publications Office,* France, April 2000.

[7] J-L. Boiffier, The Dynamics of Flight, The Equations, *SUPAÉRO(Ecole Nationale Supérieure de l'Aéronautique et de l'Espace) et ONERA-CERT,* Toulouse 25 Janvier 1999.

[8] J-L Boiffier, Dynamique de vol de l'avion, *SupAéro, Départements des Aéronefs,* Toulouse-Novembre 2001.

[9] D. L. Bricker, SQP: Sequential quadratic programming, *Dept. of Industrial Engineering, University of Iowa,* Iowa City, Iowa 52242.

[10] J. F. Bonnans, J. C. Gilbert, C. Lemarchal and C. A. Sagastizabal, Numerical Optimization: Theorical and pratical Aspects, *Springer,* p490, 2006.

[11] B. Christof and M. Helmut, SQP-methods for solving optimal control problems with control and state constraints: adjoint variables, sensitivity analysis and real-time control, *Elsivier Science, Journal of Computational and Applied Mathematics,* **120** August 2000, pp85-108.

[12] I. Chryssoverghi, J. Colestos and B. Kokkinis, Classical and relaxed optimization methods for optimal control problems *International Mathematical Forum,* 2-2007 $N°$ 30, pp 1477-1498.

[13] DGAC, Mémento à l'usage des utilisateurs des procédures d'approche et de départ aux instruments, *Rapport de la DGAC, 5ˆème édition,* Août 1995.

[14] DGAC, Méthodes et minimums de séparations des aéronefs aux procédures, *Rapport de la DGAC, 5ˆème édition,* Fevrier 2009.

[15] O. Dominique, Cisaillement de vent ou Windshear, *http://www.aviation-fr.info,* 2008.

[16] A. Filippone, Comprehensive analysis of transport aircraft flight performance, *ScinceDirect article,* **44** Manchester M60 1QD, pp 192-236 April 2008.

[17] R. Fourer, D-M. Gay and B-W. Kernigham, A modelling Language for Mathematical Programming, Second edition, *Thomson Brooks[en ligne]disponible sur http://www.ampl.com,* 2003

[18] J. C. Gilbert, SQPpro: A solver of nonlinear optimization problems, using an SQP approach, *Rapport INRIA N° 0378* Décembre 2009.

[19] J. C. Gilbert, Eléments d'optimisation différentiable - Théorie et Algorithmes, *INRIA Rocquencourt* France, 6 juin 2009.

[20] D.E. Groesbeck, R.J. Stone and C.L. Zola, An improved prediction method for noise generated by conventional profile coaxial jets, *NASA TM - 82712,* (1981), AIAA-81-1991.

[21] P.E. Gill, W. Murray and Michael A. Saunders, SNOPT: An SQP Algorithme for large-scale constrained optimizatio, *SIAM,* vol. 47, nO1, pp99-131, 2005.

[22] M-M. Harris and E. Mary, How do we Describe Aircraft Noise? *NASA TM - 82712,* FICAN,[en ligne] disponible sur www.fican.org.

[23] H. Harvey Hubbard, Aeroacoustics of flight vehicles, Theory and Practices *Volume 1: Noise sources and Volume 2: Noise Control. NASA Langley Research Center,* Hampton, Virginia 1994.

[24] Ifrance, Fiches techniques, historiques et photos d'avions A300-600, A300-600R,*[en ligne]disponible sur http://www.ifrance.com.*

[25] S. Khardi, Mathematical Model for Advanced CDA and Takeoff Procedures Minimizing Aircraft Environmental Impact, *International mathematical Forum,*vol. 5, no 36, 1747 - 1774, 2010.

[26] S. Khardi, Reduction of commercial aircraft noise emission around airports. A new environmental challenge,*European Conference of Transport Research Institutes,* vol. 1, no 4, pp 175-184, 2009.

[27] B. Laboratories, AMPL, A modelling Language for Mathematical Programming, *http://www.ampl.com,* 2003.

[28] D. Martin, Noise monitoring in the vicnity of airports,*DSNA-DTI,[electronic] avaible on http://www.dsna-dti.aviation-civile.gouv.fr,* Mai 2000.

[29] D. Martin, L'Analyse des Nuisances sonores autour des aéroports, *Revue technique numéro 58,* Mai 2000.

[30] J. T. Mathew and J. S. Wright, A feasible trust-region sequential quadratic programming algorithm, *Optimization technical report, UNIV. OF WISCONSIN,*2002

[31] F. Nahayo and S. Khardi, Les méthodes numériques appliquées en optimisation non-linéaire et en commande optimale,*Rapport LTE N° : 0911,* Novembre 2009.

[32] J Nocedal and S.J. Wright, Numerical Optimization, Second edition,*Springer Series in operations research, Springer Verlag,* 2006.

[33] R-H. Byrd, J. Nocedal and R-A. Waltz, KNITRO: An integrated Package for nonlinear optimization, *University of Colorado[en ligne]disponible sur http://www.ziena.com, http://www.ampl.com,* February, 2006

[34] M. Ouriemchi, Résolution de problèmes non-linéaires par les méthodes des points intérieurs. Théorie et algorithmes,*Thèse de l'Université de Havre*, 2005.

[35] A. Peyrat-Armandy, *Les avions de transport modernes et futurs,* TEKNEA, 1997.

[36] E. Roux, Pour une approche analytique de la dynamique du vol, *Thèse, SUPAERO-ONERA,* Novembre 2005.

[37] E. Roux, Modèle de longueur de piste au décollage-atterrissage, Avions de transport civil,*SUPAERO-ONERA,* p 345, 2006.

[38] H. Sors, Séparation et contrôle aérien, *International Virtual Aviation Organization[en ligne]disponible sur http://academy.ivao.aero/,* 15 octobre 2008

[39] V-I. Tokarev and O-I. Zapolozhets, Predicted Flight Procedures for Minimum Noise Impact, Vol 55, Numéro 2, pp129-149, Elsevier Science Ltd(Great Britain), Ukraine, 1998.

[40] M. Ventre, Les challenges environnementaux pour le transport aérien, *SAFRAN, Un leader technologique international,* Septembre 2009.

[41] T. Plantenga and R. Waltz, KNITRO 5.1 for nonlinear Optimization, Ziena Optimization, *[en ligne]disponible sur http://www.ziena.com,* Inc.May, 2007

[42] M. Xavier-Jonsson, Méthodes des points intérieurs et de régions de confience en optimisation non-linéaire et application à la conception des verres ophtamiques progressifs, *Thèse de l'Université Paris IV,* 2002.